JOURNAL OF QUATERNARY SCIENCE (2013) **28**(7) 673–682 ISSN 0267-8179. DOI: 10.1002/jqs.2666

Apparent OSL ages of modern deposits from Fåbergstølsdalen, Norway: implications for sampling glacial sediments

G. E. KING,[†]* R. A. J. ROBINSON and A. A. FINCH
Department of Earth & Environmental Sciences, University of St Andrews, Irvine Building, North Street, St Andrews, Fife KY16 9AL, Scotland, UK

Received 22 May 2013; Revised 8 September 2013; Accepted 13 September 2013

ABSTRACT: The application of optically stimulated luminescence (OSL) dating within glacial settings can be limited where sediments have not had their OSL signal fully reset by sunlight exposure. Heterogeneous bleaching can result in age overestimations, and although it is recognized that certain depositional settings are more likely to have experienced sufficient sunlight exposure to bleach the OSL signal, no comprehensive study has empirically investigated the processes of sediment bleaching, or the variability in bleaching between deposits of the same type and within the same glacial catchment. A suite of modern glacial and glaciofluvial sediments from Fåbergstølsdalen, southern Norway, have been analysed to explore the controls that sedimentary processes and depositional setting have on bleaching of the OSL signal of quartz. There is considerable variability in the residual OSL ages of similar modern deposits, which reflects high sensitivity of the OSL signal to sediment source, sedimentary process, transport distance and depositional setting. Overdispersion values are greatest for the sediments which have been most heterogeneously bleached and these sediments have the lowest residual ages. Sampling strategies that incorporate sufficient consideration of the depositional framework of sample settings can minimize the effects of unbleached residuals on OSL age determinations. Copyright © 2013 The Authors. *Journal of Quaternary Science* published by John Wiley & Sons Ltd on behalf of Quaternary Research Association

KEYWORDS: glacial environments; Norway; optically stimulated luminescence dating; sediment bleaching; transport and depositional processes.

Introduction

A major challenge to optically stimulated luminescence (OSL) dating within glacial environments is identifying sediments that have been fully exposed to sunlight, and so have had their luminescence signal fully reset (bleached). Although the effects of partial bleaching can be overcome, for example through the use of age models (e.g. Thrasher *et al.*, 2009a), understanding how depositional processes influence bleaching opportunities for sediments may enable more informed sample selection within glacial settings. Sediments have the potential to be bleached following erosion when grains are exposed to sunlight at the surface, and during waterborne and aeolian transport and deposition. Fuchs and Owen (2008) have made recommendations on the likely bleaching history of glacial and associated sediments, drawing on the literature of previous OSL applications in glacial settings. However, beyond the early work of Gemmell (1988, 1997) on the bleaching of suspended sediments from meltwater streams, only a few studies have explored the processes of sediment bleaching in glacial environments empirically (e.g. Alexanderson, 2007; Alexanderson and Murray, 2012). Alexanderson (2007) measured the OSL of six bed-load samples of ripple-laminated, sandy, longitudinal- and side-bar deposits from five different, ice-distal Greenlandic rivers. She recorded unbleached residual doses of 0.1–1 Gy for rivers draining perennial snowfields of $\geq$2 km distance from her sampling sites, which equate to residual ages of between 50 and 500 years and are similar to those reported for modern fluvial sediments (e.g. Wallinga, 2002). Alexanderson (2007) observed no variation in unbleached residuals between rivers of different channel width, depth, discharge, sediment load or sediment transport distance, but acknowledged that analysis of a downstream transect throughout a catchment would be required to elucidate the effects on sediment bleaching of these individual factors. Alexanderson and Murray (2012) sampled ice-proximal, glaciofluvial and ice-distal glaciomarine sediments; they recorded residual doses of up to 12 Gy for quartz OSL of ice-proximal deposits, whereas ice-proximal glaciomarine sediments were completely bleached.

Partial bleaching of a sediment results in a distribution of D_e values beyond that explained by random and systematic uncertainties, which is called the sample overdispersion (σ_d, Galbraith *et al.*, 1999). Overdispersion can have a range of causes (cf. Murray and Roberts, 1997; Nathan *et al.*, 2003; Olley *et al.*, 1997), but key to this research is partial or heterogeneous bleaching (Murray *et al.*, 1995). Because OSL D_e distributions are controlled by the amount of bleaching that mineral grains have been exposed to, source sediment D_e distributions are modified by the processes of erosion and sedimentation that they experience. If the D_e distributions of source sediments (e.g. subglacial or paraglacial sediments) can be well constrained, then the D_e distributions of samples from different depositional environments (e.g. glaciofluvial bars) should encode information about the bleaching that occurs during transport and depositional processes.

In the present study, the residual luminescence signals of a suite of complementary glacial sediments are investigated in a transect along a single glacial meltwater channel. Appropriate sample selection is key to obtaining accurate and precise OSL ages for glacial sediments, and this study makes several recommendations for successful sampling strategies and the identification of sediments which have been most effectively bleached.

*Correspondence: G. E. King, as above.
Email: georgina.king@unil.ch
[†]Present address: Institute of Earth Sciences, University of Lausanne, Ch-1015, Lausanne, Switzerland

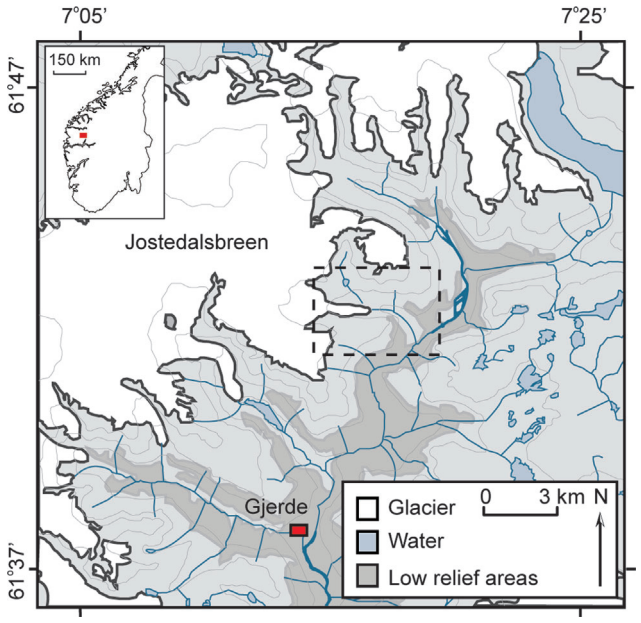

Figure 1. Map of the study area. Inset shows the location of Jostedalen in southern Norway and the dashed box shows the location of Fåbergstølsdalen. This figure is available in colour online at wileyonlinelibrary.com.

Study area and geomorphological setting

Fåbergstølsbreen is an outlet glacier from the Jostedalsbreen ice cap, the largest body of ice in mainland Europe (Fig. 1). Fåbergstølsdalen is thought to have completely deglaciated by ~8 ka cal BP (Nesje *et al.*, 1991; original 9 ka age calibrated using IntCal09 (Reimer *et al.*, 2009) assuming an uncertainty of 100 years in OxCal v.4.2 (Bronk Ramsey, 2009)), and the Jostedalsbre Plateau by 7.9–5.3 ka cal BP (Matthews *et al.*, 2000). Jostedalen has experienced significant Neoglaciation since ~5 ka cal BP and substantial advances occurred from ~3 ka (Shakesby *et al.*, 2004). The Little Ice Age (LIA, ~1750 AD) advance has been the most substantial of the Neoglacial period, and the various glaciers fed by the Jostedalsbreen ice cap have a multitude of retreat moraines related to the LIA (Dahl *et al.*, 2002). Jostedalen is within the Western Gneiss region of Norway (Bryhni and Sturt, 1985), and is underlain by bedrock of Precambrian granitic to granodioritic gneiss (Holtedahl, 1960; Holtedahl and Dons, 1960). Fåbergstølsdalen is underlain by a quartz diorite.

Fåbergstølsdalen is an E–SE-trending valley with a catchment area of ~3 km^2; vegetation is established only in the lower reaches of the catchment (Figs 2 and 3). A single meltwater stream drains Fåbergstølsbreen, which anastomoses in the lower catchment as the channel gradient reduces. The catchment is asymmetrical, with a steep (~60°) rock face comprising the north-facing valley side, whereas the south-facing valley side is less steep (~37°) and comprises large volumes of paraglacial and till deposits (Ballantyne and Benn, 1994). The paraglacial deposits are formed from subglacial material which has undergone modification in the form of debris flows and slides, and are remobilized by sheetwash processes and avalanching. These deposits are actively reworked and characterize the sediment transport and depositional processes in Fåbergstølsdalen. Debris flows are a common paraglacial process within this region (e.g. Curry and Ballantyne, 1999) and Ballantyne and Benn (1994) ascribed spring snowmelt as the key driver of paraglacial modification in Fåbergstølsdalen, in contrast to high precipitation events which have been suggested as the dominant driver for other areas of Norway (e.g. Matthews *et al.*, 1997; Sletten and Blikra, 2007).

The optical exposure history of the different subglacial and paraglacial source sediments in Fåbergstølsdalen varies, and consequently they have a range of potential residual luminescence doses. Modern material derived from paraglacial debris flows is anticipated to have high residual luminescence doses, as the rapid transit time and turbulent properties of debris flows afford limited opportunity for light exposure. Similarly, translational debris slides will only provide sunlight exposure for the sediment at the surface, and the interior part of the main slide body may see no light exposure at all. The

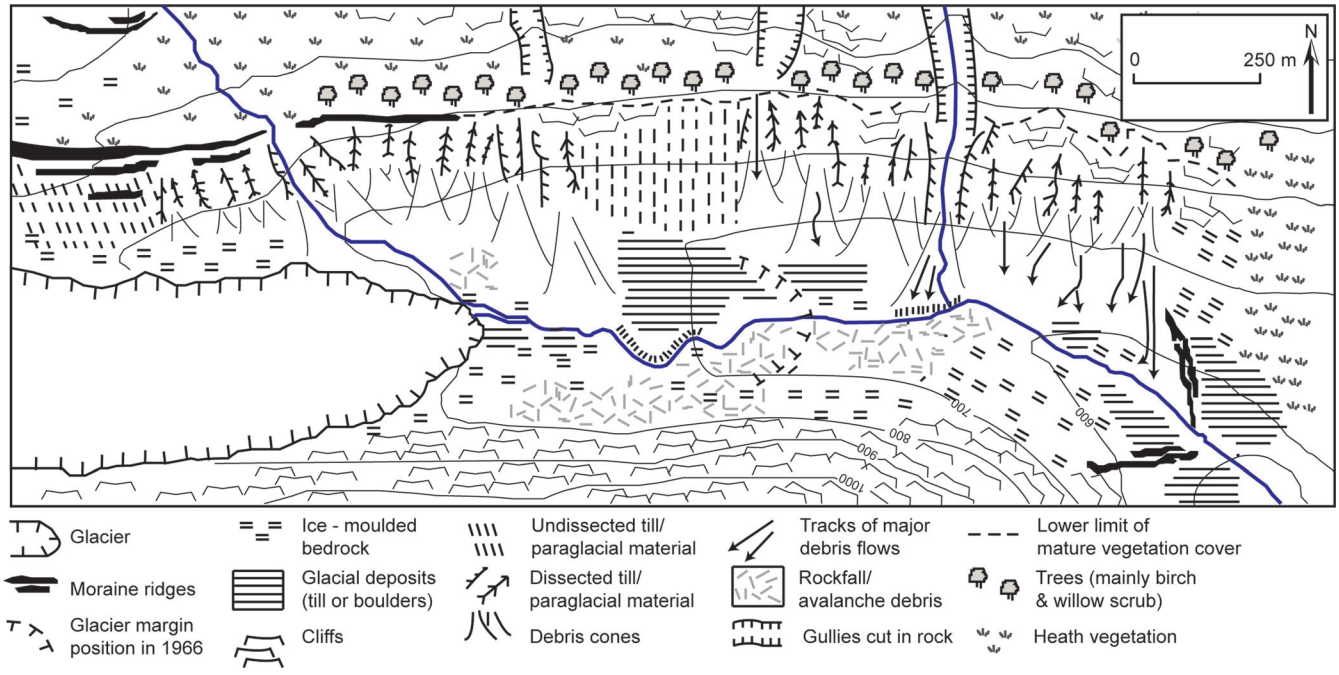

Figure 2. Geomorphological map of Fåbergstølsdalen adapted from Ballantyne and Benn (1994).

glaciofluvial bars in Fåbergstølsdalen are sourced directly from both subglacial and paraglacial sediments, and this research will enable evaluation of the influence of source sediment optical exposure histories and processes of deposition on the luminescence properties of the resultant deposits.

Sampling strategy and methods

Sample selection

A high-resolution suite of modern glacial sediments from Fåbergstølsdalen, southern Norway, have been investigated. The study of modern sediments allows the unbleached residual luminescence signals and bleaching properties of depositional processes to be investigated. Two subglacial and four paraglacial source deposits, and 11 modern glaciofluvial bar deposits were sampled throughout the catchment for OSL and grain size analyses (GSA, Table 1). Increasing transport distances have been shown to result in increased sediment bleaching in glaciofluvial environments (Gemmell, 1997). Investigation of a transect of samples throughout the catchment enables quantification of the influence of increasing transport distances on sediment bleaching in this proximal glacial setting (<2 km from ice front).

Sample modernity was determined by stratigraphic location and depositional context. Sample sites were covered with an opaque, plastic bag and a horizontal face of at least 20 mm of

Table 1. Sample depositional context and sedimentology.

Sample	Description & location	Facies*	Texture	Bedding	Scale (thickness)
Subglacial					
FAB_SUB1 FAB_SUB2	Subglacial material from beneath glacier snout	Dmm	Silt - boulders, angular - subangular, consolidated	Massive	>1 m
Paraglacial					
FAB41	Sheet wash sampled adjacent to a meltwater stream	Sh	Medium to coarse sand	Horizontal to low-angle bedding	>15 cm
FAB42	Snow avalanche debris	Dmm	Poorly sorted, coarse sand to subangular pebbles	Massive	<5 cm
FAB85	Sheet wash deposit collected 5 m above the main channel	Sh:Fl	Well-sorted sand	Horizonal bedding, units <0.5 cm	5 cm
FAB86	Sheet wash deposit collected from the confluence of a valley side tributary and the main meltwater channel	Sr	Fine to medium sand	Ripple cross bedding	5 cm
Glaciofluvial Bar					
FAB79	Bar deposit sampled adjacent to a meltwater tributary stream, north of the glacier snout	Sh	Fine to medium and medium to coarse sand layers	Low-angle cross lamination, units 1 cm thick	10 cm
FAB80	Bar deposit collected 100 m from glacier snout	Fl	Fine sand to silt, overlaying medium sand	Low-angle cross lamination, units 1 cm thick	10 cm
FAB84	Bar deposit collected from main meltwater channel	Sr	Well sorted	Ripple cross bedding, units 1 cm to 6 cm	30 cm
FAB90	Bar deposit from the lee side of a boulder adjacent to the main meltwater channel	Sh	Fine sand - silt, loosely consolidated, well sorted	Horizontal bedding, units 1 cm to 3 cm	30 cm
FAB91	Bar deposit collected from main meltwater channel	Sr	Moderately sorted, fine sand - coarse gravel	Ripple cross bedding, units vary in clast size from gravels to sands and are 1 cm to 3 cm thick	15 cm
FAB92	Bar deposit collected from main meltwater channel	Sh	Moderately sorted fine sand to gravel	Horizontal bedding, 1-cm-thick veneer of fine sand overlying coarse sand and gravel	15 cm
FAB94	Bar deposit collected from the confluence of a valley side stream and the main meltwater channel	Sh:Fl	Moderately sorted fine sand to silt	Horizontal bedding, 5-cm-thick layer of fine sand to silt overlying coarse sand and gravel	10 cm
FAB95	Bar deposit from the lee side of a boulder adjacent to the main meltwater channel	Sr	Well-sorted medium to coarse sand	Interbedded medium and coarse sand units, 2–3 cm thick	30 cm
FAB98	Bar deposit from the lee side of a boulder adjacent to the main meltwater channel	Sh	Well-sorted, medium sand	Interbedded medium and coarse sand units, 2–3 cm thick	30 cm
FAB99	Bar deposit from the main meltwater channel at the point where the valley widens and the river anastomoses.	Sh	Well-sorted, medium sand	Massive	30 cm
FAB100	Bar deposit collected from the main meltwater channel at the widest part of the valley	Sh	Well-sorted, medium sand	Massive	30 cm

*Dmm, diamicton; Sh, horizontally bedded sand; Sr, ripple bedded sand; Fl, fine laminations of sand–silt.

sediment was cleared to remove bleached surface material before sampling. Light penetration has been shown to reduce to 0.05% for coarse sand (4 mm Ø) after 7-mm depth, irrespective of wavelength (Ollerhead, 2001), and the additional ~13 mm of material removed here will account for any additional light penetration associated with loose sediment compaction. Surplus material was used for grain size analyses, which can be used to make inferences about the degree of sediment sorting throughout transport and deposition.

Luminescence sample preparation

Samples were prepared using standard OSL procedures. Material was desiccated at 50 °C to enable calculation of water content, and was sieved to extract the 180–212 μm grain size fraction. Approximately 10 g of the selected grain size was treated with 30% HCl for 30 min to remove $CaCO_3$. Samples were then treated with 30% H_2O_2 at room temperature to remove organic material. Quartz was extracted from the polymineral sample through density two separations ($\rho_1 = 2.68\,g\,cm^{-3}$, $\rho_2 = 2.58\,g\,cm^{-3}$). The 2.58–2.68 g cm^{-3} fraction was etched with 40% HF for 40 min to remove any contaminating feldspar and most of the alpha-irradiated portion of the grains. The etched quartz was treated with 30% HCl for 30 min to remove any carbonates produced during HF etching.

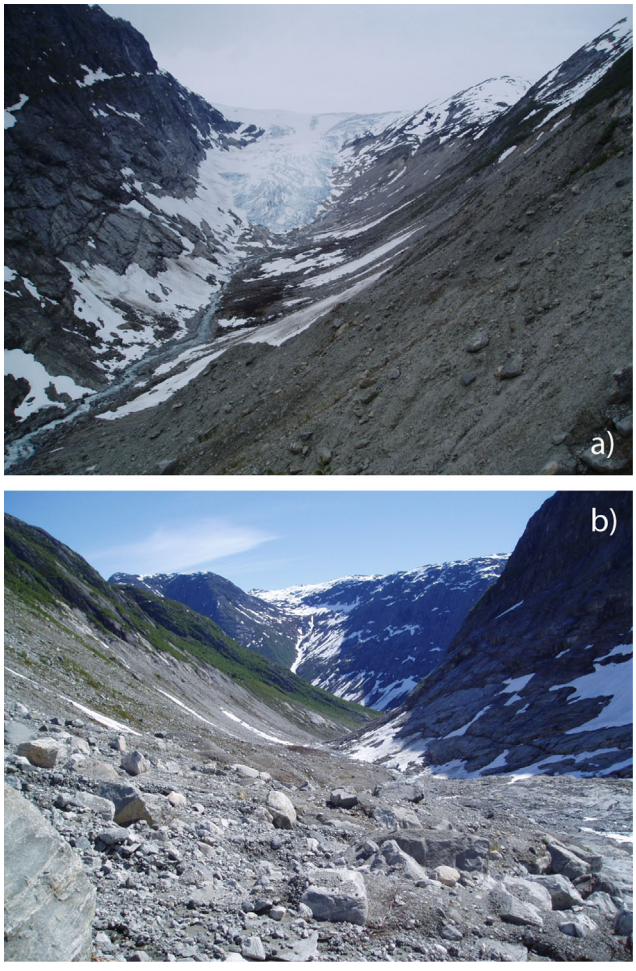

Figure 3. (a) Photograph of Fåbergstølsdalen looking up-valley (west) towards the glacier, and (b) looking down valley (east). Note the paraglacial material being reworked on the North valley side (right of photo a). This figure is available in colour online at wileyonlinelibrary.com.

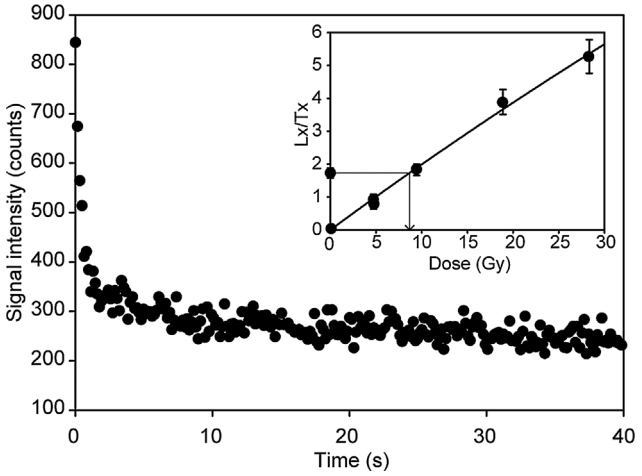

Figure 4. Natural luminescence signal decay curve of an aliquot of sample FAB85. The inset shows the luminescence dose–response curve for the same aliquot.

Luminescence measurements

All OSL measurements were carried out using either a TL-DA-15 (Bøtter-Jensen *et al.*, 2003) or TL-DA-20 Risø reader, equipped with an EMI 9235QA photomultiplier and 7.5-mm Hoya U-340 filter. Blue (470 ± 20 nm) and infrared (~870 nm) diodes were used for stimulation, and irradiation was achieved using a $^{90}Sr/^{90}Y$ beta source; dose rates were 0.1 and 0.01 Gy s^{-1} dependent on instrument. The instruments were calibrated using quartz prepared at the Risø National Laboratory in Denmark and measurements were plotted using Analyst v.3.22b (Duller, 2005). Quartz was deposited in monolayer onto stainless steel discs (9.8 mm Ø) using silicon grease; aliquot size was regulated using either a medium (5 mm Ø, ~250) or large (7 mm Ø, ~400 grain) mask.

It is not unusual for quartz from glacial environments to exhibit low luminescence sensitivity (e.g. Lukas *et al.*, 2007; Rhodes and Bailey, 1997; Richards, 2000) and the quartz analysed from Fåbergstølsdalen is dim (Fig. 4). Single-grain measurements on 400 grains of sample FAB80 carried out by Professor Geoff Duller at the Aberystwyth Luminescence Research Laboratory showed that only one grain in 400 produced a dose–response curve from which a D_e could be interpolated. The low luminescence sensitivity of these samples renders single-grain analyses unfeasible. Consequently, it is necessary for these samples to be analysed using single aliquots, although it is acknowledged that for aliquots where multiple grains contribute to the total light sum, the D_e value may be affected by averaging effects (Duller, 2008).

Luminescence analysis protocol optimization

Sample OSL signals were measured in a single aliquot regenerative dose (SAR) protocol (Murray and Wintle, 2000, Table S1, inset to Fig. 4). The temperature of preheats used in the SAR protocol was determined empirically through a dose–recovery preheat-plateau experiment on glaciofluvial bar sample FAB95. Partially bleached sediments exhibit a range of D_e values, which could mask the effects of different thermal regimes on D_e measurements. Investigation of a dose–recovery preheat-plateau test, rather than changes in natural D_e values in response to different preheating regimes, allows the challenges of partial bleaching to be circumvented. Aliquots were bleached for 60 min in direct sunlight in Lausanne on 27 July 2013, and were then given a dose of 9.5 Gy. The given dose was then measured (recovered) using

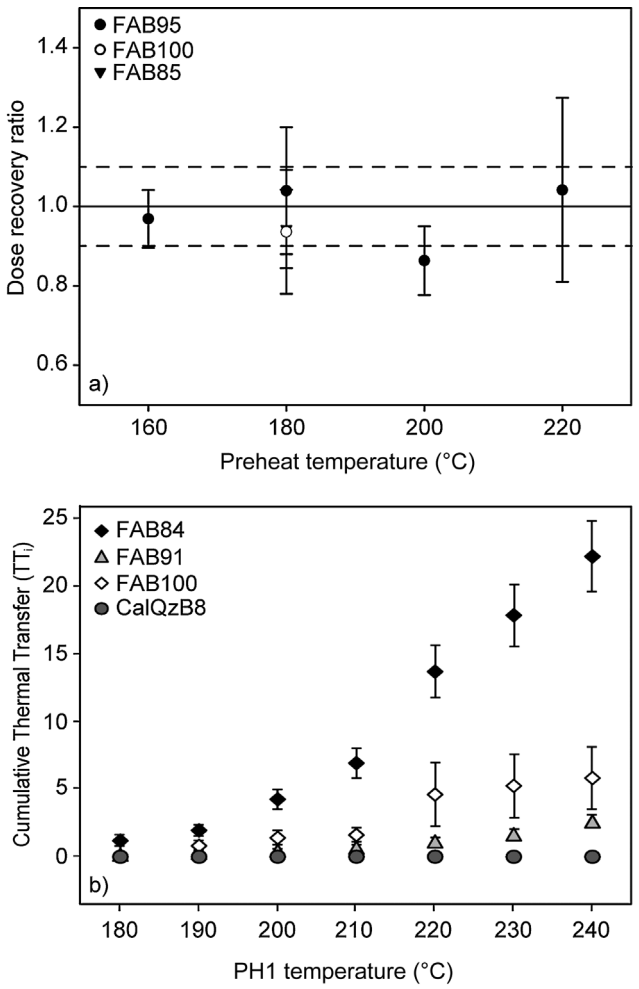

Figure 5. (a) Preheat-plateau dose–recovery data for FAB95. The solid line shows a measured dose–recovery ratio of unity and the dashed lines the 10% acceptance thresholds. The dose–recovery ratios for samples FAB85 and FAB100 in response to a 180 °C preheat are also shown. (b) Thermal transfer results for samples FAB84, FAB91 and FAB100 and a sample of Risø calibration quartz (CalQzB8) following the method of Jain *et al.* (2002).

a SAR protocol where the first and second preheat were equal (Table S1). All measurements were normalized with a test dose of 4.7 Gy, and six aliquots were measured using each of the preheat temperatures of 160, 180, 200 and 220 °C. Eleven of the measured aliquots were accepted across the four preheat temperatures, and all recovered dose within 10% of unity (Fig. 5a). Four aliquots were accepted following preheating at 160 and 180 °C, and the dose–recovery experiment was repeated on a further two samples (FAB100 and FAB85) following bleaching in direct sunlight for 60 min and preheating at 180 °C. Both samples recovered dose within 10% of unity (Fig. 5a), and therefore this protocol is regarded as appropriate for this sample suite.

Investigations into recuperation and thermal transfer of charge

Rhodes and Bailey (1997) observed that quartz in glacial systems can exhibit very dim luminescence sensitivity and may be highly susceptible to thermal transfer and recuperation. These phenomena have also been reported by other practitioners (e.g. Richards, 2000; Fuchs and Lang, 2001; Spencer and Owen, 2004; Klasen *et al.*, 2007; Lukas *et al.*, 2007; Thrasher *et al.*, 2009b). Recuperation is the non-zero luminescence response of an aliquot to zero dose, and is calculated from the zero regenerative dose point that is routinely included in SAR protocols (Table S1). As the samples analysed in this research are modern, it is inappropriate to contrast recuperation relative to the natural luminescence signal (L_n), as a zero age sample would exhibit high recuperation while potentially not suffering from the phenomenon. Instead recuperation is calculated as a percentage of the luminescence response (L_x) to the maximum regenerative dose given. Recuperation was calculated for the different aliquots of FAB95 analysed within the preheat plateau experiments, and all the rejected aliquots have recuperation $\geq$20% of the maximum regenerative dose (24 Gy).

High levels of signal recuperation can indicate thermal transfer, and this was investigated through a series of experiments to determine the proportion of transferred charge, using the experimental design of Jain *et al.* (2002). Twelve aliquots of FAB84, FAB91 and FAB100, as well as six aliquots of Batch 8 Risø calibration quartz (CalQzB8) were bleached twice with blue diodes for 100 s at room temperature, interspaced by a 1000-s pause. The 'natural' luminescence response of the bleached samples was then measured following a series of different preheat 1 (PH1) temperatures (Table S1) at 20 °C intervals from 180 to 300 °C. All L_n measurements were normalized relative to luminescence response (T_x) to a small (1 Gy) test dose which was kept low to minimize the amount of charge available for transfer during preheating. The second preheat was fixed at 180 °C. The cumulative thermally transferred (TT_i) charge is then calculated:

$$TT_i = (\Sigma N_i')/T_{180}$$

$$N_i' = N_i/\alpha$$

$$\alpha = T_i/T_{180}$$

where N_i' is the normalized luminescence signal, measured following PH1 of temperature $i_{(180–300\,°C)}$. α is calculated from normalizing T_i with T_{180}, which is the luminescence response to the test dose following measurement of N_{180}. TT_i is then calculated from the sum of N_i' over changing temperature ranges, e.g. 180–200 °C or 180–220 °C (Fig. 5b). FAB84 exhibits the greatest thermal transfer, whereas CalQz is unaffected. All samples are least affected at 180 °C, further validating the selection of this temperature for both preheats (Table S1).

Aliquot acceptance criteria used are that (1) recycling ratios (Murray and Wintle, 2000) are within 20% of unity, (2) signal intensities are $\geq 3\sigma$ above background signals, (3) IR depletion ratios are within 20% of unity (Duller, 2003), (4) D_e value uncertainties are $\leq$20% and (5) recuperation is within 10% of the normalized maximum dose. The acceptance thresholds are less stringent than normally used for dating, typically within 10% of unity for recycling ratios, and recuperation within 5% (e.g. Thrasher *et al.*, 2009b), and they have been relaxed because of the poor luminescence sensitivity of the quartz analysed (Fig. 4) and its susceptibility to thermal transfer (Fig. 5b). As all uncertainties are appropriately accounted for this does not limit the utility of this data set, other than that the precision is necessarily reduced. Causes of aliquot rejection for individual samples are listed in supplementary Table S2.

The environmental dose rate (D_r) was calculated from the concentrations of U, Th, K and Rb measured directly using inductively coupled plasma mass spectrometry (ICP-MS) and a cosmic-dose component after Prescott and Hutton (1994).

Table 2. Age-modelled D_e values, D_r values and calculated ages. The conversion factors of Adamiec and Aitken (1998) and beta particle attenuation factors after Mejdahl (1979) and Readhead (2002a, 2002b) have been used in D_r calculations; overdispersion (σ_d) values and sample skewness (c) values are also listed. All samples are modelled using the MAM-3 model with the exception of FAB92 which, due to the presence of multiple negative values, was modelled using an unlogged version of the MAM-3. An assumed Rb concentration of 100±5.00 p.p.m was also included in D_r calculations. Water content uncertainties are assumed to be 5%. The central age model (CAM) ages (Galbraith *et al.*, 1999) are provided for comparative purposes.

Sample	n	D_e (Gy)	Water content (%)	K (%)	Th (p.p.m.)	U (p.p.m.)	Wet dose rate (Gy ka^{-1})	CAM age (ka)	Age (ka)	σ_d (%)	c
Subglacial											
FABSUB1	27	2.86±1.35	10	2.85±0.17	7.68±0.38	1.69±0.09	3.51±0.21	3.45±0.70	0.81±0.39	79±12	0.57
FABSUB2	27	6.76±2.99	10	3.00±0.18	10.13±0.51	2.33±0.12	3.92±0.21	2.81±0.48	1.72±0.77	68±10	2.01
Paraglacial											
FAB41[*,†]	14	11.57±0.48	15	3.25±0.26	8.39±0.93	3.28±0.70	3.31±0.24	3.50±0.55	3.31±0.24	–	0.00
FAB42	32	0.74±0.24	28	3.59±0.21	14.44±0.72	2.71±0.14	3.63±0.22	0.80±0.15	0.20±0.07	91±11	3.10
FAB85	25	1.44±0.61	11	2.91±0.19	10.83±0.54	3.85±0.22	3.75±0.22	1.35±0.26	0.39±0.16	87±12	1.69
FAB86	36	2.84±1.99	21	3.00±0.18	7.65±0.38	3.03±0.18	3.18±0.19	3.91±0.77	0.89±0.63	91±12	0.69
Glaciofluvial bar											
FAB79	28	13.41±3.32	17	2.77±0.16	8.02±0.47	3.89±0.20	3.30±0.19	7.66±0.88	4.06±1.04	47±5	4.00
FAB80[*,†]	19	5.56±1.46	22	3.25±0.26	8.39±0.93	3.28±0.70	3.39±0.25	3.42±0.48	1.64±0.45	–	0.74
FAB84	21	4.22±1.25	13	3.22±0.19	8.47±0.42	3.47±0.17	3.72±0.23	5.75±1.08	1.13±0.34	84±13	0.95
FAB90[*]	19	10.31±3.89	14	3.04±0.01	8.65±0.12	4.15±0.09	3.66±0.22	5.38±0.75	2.82±1.08	–	0.13
FAB91	33	5.25±1.02	8	3.53±0.02	7.03±0.13	2.64±0.03	3.93±0.25	2.77±0.40	1.34±0.28	67±7	0.28
FAB92[‡,†]	29	0.00±0.37	11	3.25±0.26	8.39±0.93	3.28±0.70	3.73±0.28	1.03±0.19	0.00±0.10	0±0	−0.37
FAB94	43	5.69±1.42	20	3.14±0.18	7.87±0.39	4.06±0.46	3.48±0.21	4.55±0.56	1.64±0.42	64±6	2.61
FAB95[†]	57	8.52±2.17	16	3.25±0.26	8.39±0.93	3.28±0.70	3.61±0.27	6.12±0.72	2.36±0.63	61±5	0.94
FAB98	43	3.13±0.80	12	3.16±0.1	8.63±0.13	3.41±0.07	3.72±0.22	5.73±2.11	0.84±0.22	77±8	0.95
FAB99	32	5.96±2.11	9	3.37±0.05	7.50±0.01	3.68±0.07	3.99±0.24	2.75±0.40	1.50±0.54	50±7	0.74
FAB100	28	2.24±0.98	20	3.22±0.05	8.62±0.02	3.22±0.01	3.46±0.29	2.60±0.45	0.65±0.29	83±11	1.12

Gamma dose rates have been adjusted to account for the surface proximal location of all the samples with the exception of FABSUB1 and FABSUB2. The factors presented in table H.1 of Aitken (1985) have been used assuming a sample depth below the surface of 3 cm (i.e. the mid-point of the sample) and a soil density of 2 g cm^{-3}. [*]σ_d has not been calculated where $n < 20$. [†]Average D_r used; see text for details. [‡]6.0 Gy was added to each D_e value, to remove all negative values to calculate sample σ_d.

External alpha dose rates were ignored and no internal alpha dose contribution has been incorporated (Table 2). It was not possible to calculate D_r for four samples and instead the radioisotope values of all the Fåbergstølsdalen samples have been averaged to provide their approximate residual ages (Table 2).

Determination of residual luminescence ages

The samples analysed display heterogeneous bleaching and the D_e distributions are over-dispersed (Fig. 6). A single residual D_e value has been calculated through age modelling to make comparisons between the different samples. The model selection criteria of Bailey and Arnold (2006), with revised critical values from Arnold (2006) after Thrasher *et al.* (2009b), have been used, and all samples are modelled with the three-component minimum age model (MAM-3, assumed σ_d 10%; Galbraith *et al.*, 1999) in R 2.14.1 (R Development Core Team, 2011). Deriving residual D_e estimates from modern samples allows potential OSL age overestimations to be evaluated for the different glacial and paraglacial deposits. Sample acceptance rates vary and three samples with $n < 20$ have been rejected (King, 2012; Table 2; Table S2).

Grain size analyses

Grain size analyses were done using a Coulter LS230 laser granulometer. Bulk material was not available for all samples either due to low sediment availability for dating, or where all bulk material had been prepared for ICP-MS analysis. Material sufficient to result in 8–9% obscuration of the laser (0.5–1 g) was analysed, and duplicate analyses were made of all samples. Where deviation between initial and secondary analyses was observed, the sample was analysed a third time and particle size data were averaged. Statistics were calculated using GRADISTAT (Blott and Pye, 2001 after Folk and Ward, 1957) and the results are given in Table S3.

Results

Source deposits: subglacial and paraglacial material

The two subglacial till samples (FABSUB1 and FABSUB2) comprise diamicton, and were sampled *in situ* from beneath the snout of Fåbergstølsbreen (Table 1). Both samples have an overdispersion of ∼70 ± 10% (Fig. 7), residual ages of 0.81 ± 0.39 ka and 1.72 ± 0.77 ka, and positively skewed D_e distributions, indicative of partial bleaching (Fig. 6a; Table 2). Grain size analyses indicate that the subglacial deposits are poorly sorted and skewed towards coarser material (Table S3).

The paraglacial sediments investigated comprise subglacial till deposits which have been modified by paraglacial processes following the retreat of Fåbergstølsbreen after the LIA (Dahl *et al.*, 2002). Consequently, the paraglacial deposits within the catchment should have ages younger than ∼1750 AD. The residual ages of the paraglacial deposits are

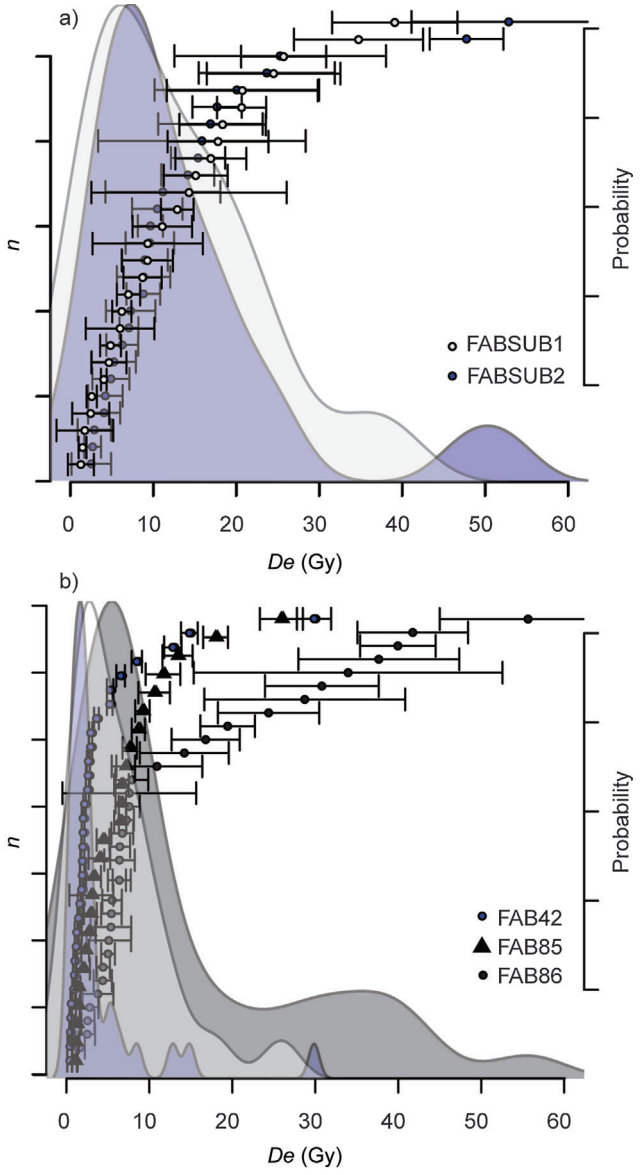

Figure 6. D_e values and probability density functions of (a) subglacial samples FABSUB1 and 2, and (b) paraglacial samples FAB42 (avalanche), FAB85 and FAB86 (sheetwash). This figure is available in colour online at wileyonlinelibrary.com.

generally younger than the subglacial deposits (Fig. 8a) and are broadly similar to one another, ranging from 200 ± 70 years for FAB42 (avalanche) to 890 ± 630 years for FAB86 (sheetwash). The increased bleaching of the paraglacial deposits relative to the subglacial sediments is reflected in their grain size analysis characteristics: although the paraglacial sediments remain poorly sorted (Table S3), they are better sorted than the subglacial deposits, exemplified by mesokurtic, rather than leptokurtic, grain size distributions.

In contrast to the subglacial sediments, the three paraglacial samples with $n > 20$ have overdispersion values of $90 \pm 10\%$ which is consistent for material reworked by different slope failure processes; for example, FAB42 comprises avalanche debris whereas FAB85 and FAB86 are sheetwash deposits (Table 1).

Glaciofluvial bar deposits

Within Fåbergstølsdalen, the glacial meltwater stream accesses both subglacial and paraglacial sediments, and both deposit types are source sediments for the glaciofluvial bars formed within the catchment. As the paraglacial sediments comprise modified subglacial material, it may be difficult to differentiate between bar sediments sourced from *in situ* subglacial deposits, and paraglacial deposits from the south-facing valley side (Fig. 7) using either their luminescence or GSA properties. Eleven samples were taken from bar deposits at increasing distances from the glacial snout (Fig. 7) and nine have aliquot acceptance rates of $n > 20$.

All samples with the exception of FAB79 were taken from similar scale bar features along the main meltwater channel. The facies of the bar deposits range from ripple (Sr) and horizontally bedded (Sh) sands, to finely laminated sands and silts (Sh:Fl), and further information on their specific sedimentology and depositional settings is given in Table 1. All the samples have GSA characteristics similar to the paraglacial deposits (Table S3), which is a consequence of the high hillslope-channel connectivity of Fåbergstølsdalen (Fig. 2).

FAB79 has a slightly different depositional setting from the other bar samples analysed: it is sampled from a tributary meltwater channel to the north of Fåbergstølsbreen, which directly accesses subglacial material and recently exposed till (Fig. 7). In comparison with the other bar deposits sampled from the main meltwater channel, FAB79 has similar GSA properties but higher residual age (4.06 ± 1.04 ka) and reduced overdispersion ($\sigma_d = 47 \pm 5\%$). These attributes are similar to the *in situ* subglacial sediments sampled, and reflect that this deposit is predominantly sourced from subglacial material (inferred from its sample location) which has been only moderately reworked during fluvial transportation over a limited distance of tens of metres.

The remainder of the glaciofluvial bar samples are all derived from similar scale features along the main Fåbergstølsdalen meltwater channel. Sediments are sourced from a mixture of subglacial and paraglacial sediments, which will contribute to deposits in different proportions depending upon the specific sampling location. FAB91, FAB95 and FAB94 are all sampled from the same locality (Fig. 7), and have similar residual ages ranging from 1.34 ± 0.28 to 2.36 ± 0.63 ka, similar overdispersion values ranging from 61 ± 5 to $67 \pm 7\%$ and similar D_e distributions (Fig. 9). The similarities between these samples suggest common source sediments and processes of transport and deposition; however, FAB92 is also sampled from a bar feature between FAB91 and FAB95, and is the only sample which is almost completely bleached (Fig. 9). This sample has zero overdispersion and 30% of aliquots for FAB92 have negative D_e values. FAB92 is also the only negatively skewed sample (Table 2), which may relate to a different controlling influence on the D_e distribution, such as the bleaching limit of the quartz. As the depositional location of this sample is similar to that of FAB91, FAB95 and FAB94, it is surprising that the luminescence properties are so different. FAB92 comprises a thin veneer of fine sand overlying gravels (Table 1), and thus material deposited at this site may have been exposed to sunlight for longer, resulting in more complete bleaching before covering by additional sediments during subsequent high flow phases.

FAB100 is the glaciofluvial bar sample taken farthest from the glacial snout (1.5 km) and has no direct subglacial or paraglacial inputs (Fig. 7). It has one of the youngest residual ages of the bar deposits: 0.65 ± 0.29 ka. It is interesting that despite the longer transport distance for material deposited at the FAB100 sample location, its overdispersion is high ($\sigma_d = 83 \pm 11\%$) in comparison with many of the other bar deposits analysed within the lower catchment (e.g. FAB91, $\sigma_d = 67 \pm 7\%$; Fig. 7). Sample FAB100 is located 250 m from the nearest potential paraglacial source sediment input into

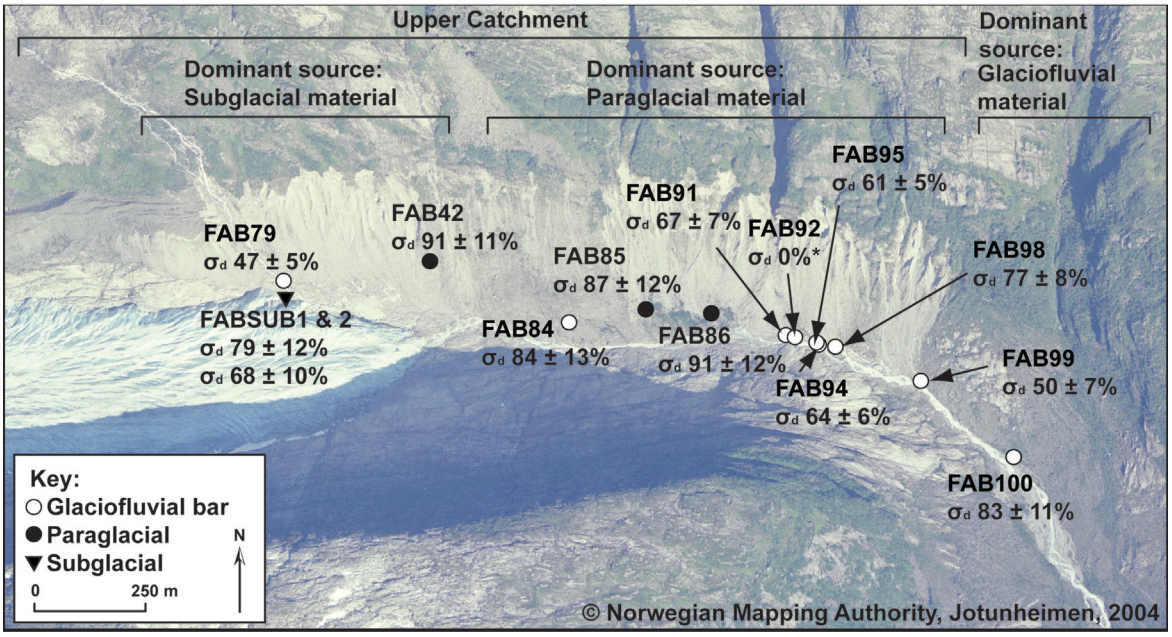

Figure 7. Aerial photograph from www.norgeibilder.no of Fåbergstølsdalen highlighting sample locations and overdispersion values. The dominant sediment sources, inferred from the catchment geomorphology, are indicated. This figure is available in colour online at wileyonlinelibrary.com.

the meltwater stream. However, it is apparent from Fig. 9 that despite the relatively long transport distance of FAB100 in contrast to the other bar samples (e.g. FAB91), its D_e distribution has been modified only slightly relative to the source deposit D_e distributions (Fig. 6).

Discussion

The residual ages of the subglacial sediments are younger than anticipated for *in situ* deposits, which should have an estimated minimum age of ~5 ka associated with the onset of Neoglaciation (e.g. Shakesby *et al.*, 2004). Material was gathered at the glacier snout due to logistical constraints and some sunlight exposure due to sediment reworking by meltwater may have occurred before sample collection. Alternatively, some of the grains analysed may be derived from supraglacial sediment which has been washed beneath the glacier. Swift *et al.* (2010) have also recently proposed that low D_e values may be attributed to signal bleaching by intense pressure and shear stresses at the glacier bed (triboluminescence).

The paraglacial samples analysed have low residual ages relative to both the subglacial and the glaciofluvial bar deposits, showing that these deposits have been recently reworked and that paraglacial processes result in more effective bleaching of OSL signals (Fig. 8a). It is surprising that the paraglacial deposits have smaller residuals than almost all the glaciofluvial bar deposits, and reflects that bleaching opportunities vary depending upon both specific depositional process and setting.

Glaciofluvial bar deposits were selected along a transect through Fåbergstølsdalen, at increasing distances from the glacial snout. It has been shown in other fluvial and glaciofluvial settings that increasing transport distances result

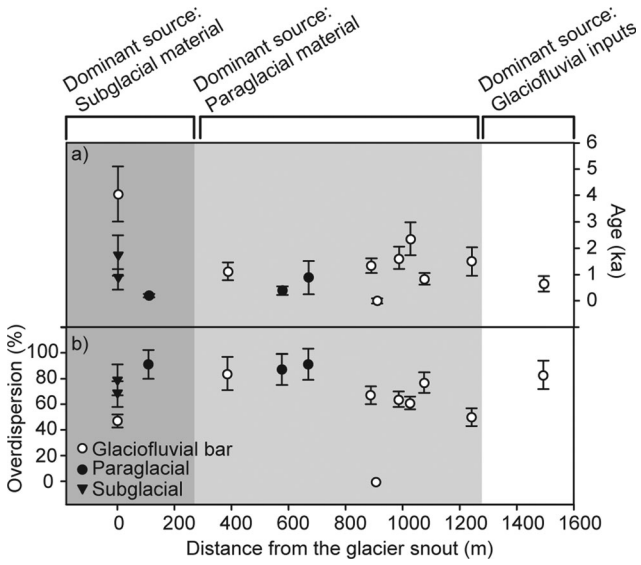

Figure 8. (a) Changing age-modelled residual ages and (b) overdispersion values for the different deposits. Dominant sediment sources, inferred from the catchment geomorphology, are indicated.

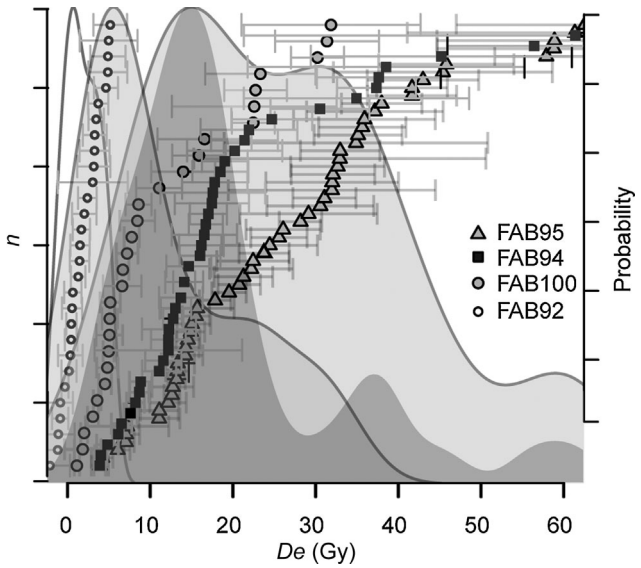

Figure 9. D_e values and probability density functions of four bar deposits sampled from Fåbergstølsdalen. The number of accepted aliquots varied between samples (Table 2) and the probability estimates are given in arbitrary units to facilitate plotting on a comparable scale.

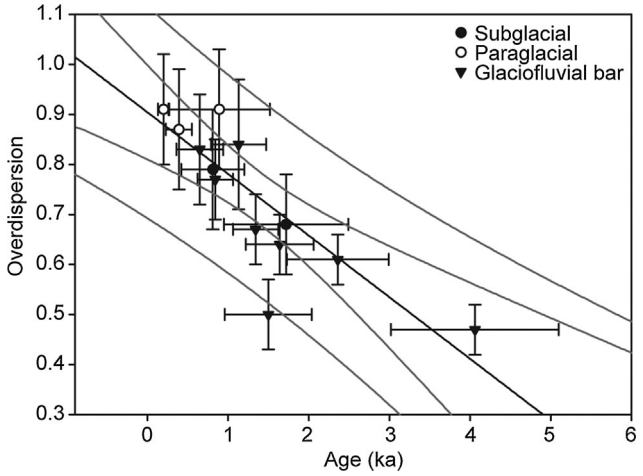

Figure 10. Correlation of residual age and overdispersion for all samples, except FAB92 which has zero age and zero overdispersion. Fitting the data with a linear regression results in an r^2 value of 0.69. The 95 and 99% confidence limits of the fit are shown.

in improved opportunities for sediment bleaching (e.g. Forman and Ennis, 1992; Stokes *et al.*, 2001). However, although a slight reduction in residual ages is recorded for the glaciofluvial bar deposits after 900 m distance from the glacial snout (Fig. 8a), the residual ages of the bar deposits are still within uncertainties of the subglacial source sediments and range from zero to 2.82 ± 1.08 ka. Contrasting the D_e distributions of the bar deposits with the subglacial and paraglacial source sediment D_e distributions (Figs 6 and 9) shows that similar ranges of D_e values are retained between the different deposit types. The properties of the source subglacial and paraglacial sediments are therefore retained over short (<2 km) transport distances, demonstrating that when sampling for conventional OSL dating applications, consideration of the source sediment properties as well as depositional processes and specific depositional setting are crucial in evaluating whether a sediment is likely to have been fully bleached. This is especially important where deposits are sampled within 2 km of the ice margin.

The subglacial source deposits have overdispersion values of ~70%, which are similar to the bar deposits but lower than the paraglacial sediments (Fig. 8b). If the residual ages of the different deposits are also considered, as the paraglacial deposits analysed have the smallest residual ages, it can be inferred that higher overdispersion values indicate improved (but incomplete) sediment bleaching. If the overdispersion values of the different subglacial, paraglacial and bar deposits are plotted relative to their residual ages (excluding sample FAB92, which is completely bleached), a correlation with r^2 of 0.69 is obtained (Fig. 10), demonstrating that for these sediments, high overdispersion values indicate the greatest degree of signal resetting. This has implications for dating glacial sediments as overdispersion values encode information of the degree of sediment bleaching, providing an additional tool through which the suitability of a sample can be assessed. Further work is required to investigate the range of overdispersion values recorded for other glacial deposits and depositional processes from a range of different glacial environments to understand this relationship more fully.

Conclusions

The luminescence properties of a suite of glacial sediments within 2 km of the ice margin from a single glacial catchment from southern Norway have been characterized to quantify residual ages and investigate the processes of sediment bleaching. The subglacial and paraglacial sediments investigated form the source sediments of the glaciofluvial bar deposits analysed, and the paraglacial sediments have the smallest residual ages but the greatest overdispersion values. The residual ages of most of the glaciofluvial bar deposits range from zero to 2.82 ± 1.08 ka and are within uncertainties of the subglacial sediment residual ages. Changing overdispersion values between the different deposits indicates that transport and depositional processes modify overdispersion because of sediment bleaching, and deposits with the greatest overdispersion values have experienced the greatest bleaching (while remaining partially reset). Grains transported by the same processes of sedimentation have different residual ages dependent upon the duration of transport, the sediment source and specific depositional setting. This has implications for studies reliant on the use of a single modern analogue deposit, which may underestimate or overestimate likely residual doses. The analysis of multiple modern analogue deposits, while time-consuming, would enable better constraint of the range of residual doses, which vary by almost 3 ka for the glaciofluvial bar deposits analysed in this study. Consideration of the depositional framework of an OSL sample should also be used to reduce the risk of sampling a deposit which suffers from partial bleaching.

Supporting Information

Additional supporting information can be found in the online version of this article:

Table S1. Quartz SAR protocol.

Table S2. Causes of aliquot rejection for individual samples.

Table S3. Moment particle size analysis results after Folk and Ward (1957) calculated in GRADISTAT (Blott and Pye, 2001).

Acknowledgements. G. E. K. was supported by NERC studentship F008589/1 and was affiliated to SAGES. R. Galbraith is thanked for providing the R code for the age models. R. Sommerville, A. Calder and D. Herd (University of St Andrews) and L. Carmichael and S. Fisk (SUERC) are thanked for laboratory assistance. D. Sanderson (SUERC) is thanked for useful discussions, and for access to facilities. D. Lowry (University of St Andrews), E. Harris (Swansea University), L. Baek Nielsen, C. Caballero and A. Cullens (IceTroll) are thanked for fieldwork assistance. A New Workers Research Award is acknowledged from the QRA. P. Abbott (Swansea University), A. Rowan and R. Smedley (Aberystwyth University) and two anonymous reviewers are thanked for comments on an earlier version of this manuscript.

Abbreviations. GSA, grain size analysis; ICP-MS, inductively coupled plasma mass spectrometry; LIA, Little Ice Age; OSL, optically stimulated luminescence; SAR, single aliquot regenerative dose

References

Adamiec G, Aitken MJ. 1998. Dose-rate conversion factors: update. *Ancient TL* **16**: 37–46.

Aitken MJ. 1985. *Thermoluminescence Dating*. Academic Press: London.

Alexanderson H. 2007. Residual OSL signals from modern Greenlandic river sediments. *Geochronometria* **26**: 1–9.

Alexanderson H, Murray AS. 2012. Luminescence signals from modern sediments in a glaciated bay, NW Svalbard. *Quaternary Geochronology* **10**: 250–256.

Arnold LJ. 2006. Optical dating and computer modelling of arroyo epicycles in the American Southwest. DPhil Thesis, St Peter's College, University of Oxford.

Bailey RM, Arnold LJ. 2006. Statistical modelling of single grain quartz D-e distributions and an assessment of procedures for estimating burial dose. *Quaternary Science Reviews* **25**: 2475–2502.

Ballantyne CK, Benn DI. 1994. Paraglacial slope adjustment and resedimentation following recent glacier retreat, Fåbergstølsdalen, Norway. *Arctic and Alpine Research* **26**: 255–269.

Blott SJ, Pye K. 2001. GRADISTAT: a grain size distribution and statistics package for the analysis of unconsolidated sediments. *Earth Surface Processes and Landforms* **26**: 1237–1248.

Bøtter-Jensen L, Andersen CE, Duller GAT, *et al*. 2003. Developments in radiation, stimulation and observation facilities in luminescence measurements. *Radiation Measurements* **37**: 535–541.

Bronk Ramsey C. 2009. Bayesian analysis of radiocarbon dates. *Radiocarbon* **51**: 337–360.

Bryhni I, Sturt BA. 1985. Caledonides of southwestern Norway. In *The Caledonide Orogen*, Gee DE, Sturt BA (eds). John Wiley & Sons: Chichester; 619.

Curry AM, Ballantyne CK. 1999. Paraglacial modification of glacigenic sediment. *Geografiska Annaler, Series A: Physical Geography* **81**: 409–419.

Dahl SO, Nesje A, Lie Ø, *et al*. 2002. Timing, equilibrium-line altitudes and climatic implications of two early-Holocene glacier readvances during the Erdalen Event at Jostedalsbreen, western Norway. *Holocene* **12**: 17–25.

Duller GAT. 2003. Distinguishing quartz and feldspar in single grain luminescence measurements. *Radiation Measurements* **37**: 161–165.

Duller GAT. 2005. *Luminescence Analyst*. University of Wales: Aberystwyth.

Duller GAT. 2008. Single-grain optical dating of Quaternary sediments: why aliquot size matters in luminescence dating. *Boreas* **37**: 589–612.

Folk RL, Ward WC. 1957. Brazos River bar: a study in the significance of grain size parameters. *Journal of Sedimentary Petrology* **27**: 3–26.

Forman SL, Ennis G. 1992. Limitations of thermoluminescence to date waterlain sediments from glaciated fiord environments of western Spitsbergen, Svalbard. *Quaternary Science Reviews* **11**: 61–70.

Fuchs M, Lang A. 2001. OSL dating of coarse-grain fluvial quartz using single-aliquot protocols on sediments from NE Peloponnese, Greece. *Quaternary Science Reviews* **20**: 783–787.

Fuchs M, Owen LA. 2008. Luminescence dating of glacial and associated sediments: review, recommendations and future directions. *Boreas* **37**: 636–659.

Galbraith RF, Roberts RG, Laslett GM, *et al*. 1999. Optical dating of single and multiple grains of quartz from jinmium rock shelter, northern Australia, Part 1, Experimental design and statistical models. *Archaeometry* **41**: 339–364.

Gemmell AMD. 1988. Thermoluminescence dating of glacially transported sediments – some considerations. *Quaternary Science Reviews* **7**: 277–285.

Gemmell AMD. 1997. Fluctuations in the thermoluminescence signal of suspended sediment in an Alpine glacial meltwater stream. *Quaternary Science Reviews* **16**: 281–290.

Holtedahl O. 1960. *Geology of Norway*. I Kommisjon Hos H. Aschehoug, & Co.: Oslo.

Holtedahl O, Dons JA. 1960. Geologisk kart over Norge Berggrunnskart. Norges Geologiske Undersøkelse Nr. 208: Oslo.

Jain M, Bøtter-Jensen L, Murray AS, *et al*. 2002. Retrospective dosimetry: dose evaluation using unheated and heated quartz from a radioactive waste storage building. *Radiation Protection Dosimetry* **101**: 525–530.

King GE. 2012. Fundamental and Sedimentalogical Controls on the Luminescence of Quartz and Feldspar. PhD Thesis, University of St Andrews.

Klasen N, Fiebig M, Preusser F, *et al*. 2007. Luminescence dating of proglacial sediments from the Eastern Alps. *Quaternary International* **164–165**: 21–32.

Lukas S, Spencer JQG, Robinson RAJ, *et al*. 2007. Problems associated with luminescence dating of Late Quaternary glacial sediments in the NW Scottish Highlands. *Quaternary Geochronology* **2**: 243–248.

Matthews JA, Dahl SO, Nesje A, *et al*. 2000. Holocene glacier variations in central Jotunheimen, southern Norway based on distal glaciolacustrine sediment cores. *Quaternary Science Reviews* **19**: 1625–1647.

Matthews JA, Dahl SO, Berrisford MS, *et al*. 1997. A preliminary history of Holocene colluvial (debris-flow) activity, Leirdalen, Jotunheimen, Norway. *Journal of Quaternary Science* **12**: 117–129.

Mejdahl V. 1979. Thermoluminescence dating: beta-dose attenuation in quartz grains. *Archaeometry* **21**: 61–72.

Murray AS, Olley JM, Caitcheon GG. 1995. Measurement of equivalent doses in quartz from contemporary water-lain sediments using optically stimulated luminescence. *Quaternary Science Reviews* **14**: 365–371.

Murray AS, Roberts RG. 1997. Determining the burial time of single grains of quartz using optically stimulated luminescence. *Earth and Planetary Sciences Letters* **152**: 163–180.

Murray AS, Wintle AG. 2000. Luminescence dating of quartz using an improved single-aliquot regenerative-dose protocol. *Radiation Measurements* **32**: 57–73.

Nathan RP, Thomas PJ, Jain M, *et al*. 2003. Environmental dose rate heterogeneity of beta radiation and its implications for luminescence dating: Monte Carlo modelling and experimental validation. *Radiation Measurements* **37**: 305–313.

Nesje A, Kvamme M, Rye N, *et al*. 1991. Holocene glacial and climate history of the Jostedalsbreen region, Western Norway; evidence from lake sediments and terrestrial deposits. *Quaternary Science Reviews* **10**: 87–114.

Ollerhead J. 2001. Light transmittance through dry, sieved sand: some test results. *Ancient TL* **19**: 13–17.

Olley JM, Roberts RG, Murray AS. 1997. Disequilibria in the uranium decay series in sedimentary deposits at Allen's Cave, Nullarbor Plain, Australia: implications for dose rate determinations. *Radiation Measurements* **27**: 433–443.

Prescott JR, Hutton JT. 1994. Cosmic ray contributions to dose rates for luminescence and ESR dating: Large depths and long-term time variations. *Radiation Measurements* **23**: 497–500.

R Development Core Team. 2011. R: A language and environment for statistical computing. R Foundation for Statistical Computing: Vienna.

Readhead ML. 2002a. Absorbed dose fraction for ^{87}Rb β particles. *Ancient TL* **20**: 25–28.

Readhead ML. 2002b. Addendum to 'absorbed dose fraction for ^{87}Rb β particles'. *Ancient TL* **20**: 47.

Reimer PJ, Baillie MGL, Bard E, *et al*. 2009. IntCal09 and Marine09 radiocarbon age calibration curves, 0–50,000 years cal BP. *Radiocarbon* **51**: 1111–1150.

Rhodes EJ, Bailey RM. 1997. The effect of thermal transfer on the zeroing of the luminescence of quartz from recent glaciofluvial sediments. *Quaternary Science Reviews* **16**: 291–298.

Richards BWM. 2000. Luminescence dating of Quaternary sediments in the Himalaya and High Asia: a practical guide to its use and limitations for constraining the timing of glaciation. *Quaternary International* **65–66**: 49–61.

Shakesby RA, Matthews JA, Winkler S. 2004. Glacier variations in Breheimen, southern Norway: relative-age dating of Holocene moraine complexes at six high-altitude glaciers. *Holocene* **14**: 899–910.

Sletten K, Blikra LH. 2007. Holocene colluvial (debris-flow and water-flow) processes in eastern Norway: stratigraphy, chronology and palaeoenvironmental implications. *Journal of Quaternary Science* **22**: 619–635.

Spencer JQ, Owen LA. 2004. Optically stimulated luminescence dating of Late Quaternary glaciogenic sediments in the upper Hunza valley: validating the timing of glaciation and assessing dating methods. *Quaternary Science Reviews* **23**: 175–191.

Stokes S, Bray HE, Blum MD. 2001. Optical resetting in large drainage basins: tests of zeroing assumptions using single-aliquot procedures. *Quaternary Science Reviews* **20**: 879–885.

Swift DA, Sanderson DCW, Nienow PW, *et al*. 2010. Anomalous luminescence of subglacial sediment at Haut Glacier d'arolla, Switzerland – a consequence of resetting at the glacier bed? *Boreas* **40**: 446–458.

Thrasher IM, Mauz B, Chiverrell RC, *et al*. 2009a. Luminescence dating of glaciofluvial deposits: a review. *Earth-Science Reviews* **97**: 145–158.

Thrasher IM, Mauz B, Chiverrell RC, *et al*. 2009b. Testing an approach to OSL dating of Late Devensian glaciofluvial sediments of the British Isles. *Journal of Quaternary Science* **24**: 785–801.

Wallinga J. 2002. Optically stimulated luminescence dating of fluvial deposits: a review. *Boreas* **31**: 303–322.